Dielectric measurements in highly deuterated betaine phosphite

Joachim Hemberger, Peter Lunkenheimer, H. Ries, A. Maiazza, Alois Loidl

Angaben zur Veröffentlichung / Publication details:

Hemberger, Joachim, Peter Lunkenheimer, H. Ries, A. Maiazza, and Alois Loidl. 1996. "Dielectric measurements in highly deuterated betaine phosphite." *Ferroelectrics* 175 (1): 153–63. https://doi.org/10.1080/00150199608213384.

DIELECTRIC MEASUREMENTS IN HIGHLY DEUTERATED BETAINE PHOSPHITE

J. HEMBERGER, P. LUNKENHEIMER, H. RIES, A. MAIAZZA and A. LOIDL
Institut für Festkörperphysik, Technische Hochschule Darmstadt, D-64289 Darmstadt, Germany

We have performed a detailed investigation of the dielectric properties of deuterated betaine phosphite (D-BPI) using broadband dielectric spectroscopy, measurements of the non-linear susceptibility, of the pyroelectric coefficient, and of the field dependent polarization. D-BPI becomes ferroelectric in two successive phase transitions at T_{c2} = 272 K and T_{c3} = 266 K. At frequencies $\nu > 100$ MHz a critical slowing down of the order dynamics at 266 K could be observed. In addition, we found evidence for a third polar phase transition at T_{c4} = 250 K. At temperatures around 150 K a relaxational process, most probably due to domain wall motions, shows up which is highly field dependent with an energy barrier of 5300 K at low fields.

1. INTRODUCTION

The addition compounds of the α-amino acid betaine with several adducts like arsenate, phosphate or phosphite form a group of complex crystals with interesting dielectric properties. Since the first observations of order transitions in these materials,[1] this family of crystals and mixed crystals has been the subject of many investigations. A broad spectrum of different ordering behaviours has been found: Protonated betaine arsenate (BA) and betaine phosphite (BPI) show ferroelectric behaviour,[2-4] while protonated (BP) as well as deuterated betaine phosphate (D-BP) exhibit antiferroelectric transitions.[1,5] Deuterated betaine arsenate (D-BA) even shows a sequence of antiferro- and ferroelectric transitions.[6] Finally, betaine calcium chloride dihydrate (BCCD) reveals a variety of subsequent commensurate and incommensurate phases.[7] Additional interest in this class of materials stems from the fact, that their structural isomorphism enables the growth of mixed crystals. Here competing dipole-dipole interactions supress polar order and drive an orientational glass transition.[8] The present work deals with deuterated betaine phosphite, $(CH_3)_3NCH_2COO \cdot D_3PO_3$ (D-BPI).

In analogy to the protonated compounds[3,9] it can be concluded, that the inorganic PO_3 group is connected via a hydrogen bridge to the organic betaine complex. Neighbouring phosphite groups are interconnected via the DPO_3-tedrahedra with O . . . D—O bonds along quasi one dimensional zig-zag chains, with one bond along (010) axis, and one hydrogen bridge perpendicular to it, along (101). In the ferroelectric (FE) state of betaine phosphite the FE order is achieved via the order of the protons along the b-axis, while the hydrogen bonds along (101) are arranged to avoid the formation of PO_3 groups.[9] This means that the two inequivalent protons along the quasi-linear chain are never attached to the same HPO_3 group, a fact that must introduce strong correlations of the protons in the paraelectric state and implies that

the two inequivalent protons order at the same temperature. That the protons in BPI, indeed, order at the same temperature has been demonstrated unambiguously by Electron Nuclear Double Resonance (ENDOR) experiments.[10] So far only very little is known about D-BPI. Concerning the dielectric properties, the complex dielectric constant ε^* has been measured at 5.2 kHz for temperatures 4 K $\leq T \leq$ 250 K and a weak loss peak has been reported.[11] Here we present a detailed dielectric investigation of D-BPI, including broadband dielectric spectroscopy, field, frequency and temperature dependence of the nonlinear susceptibility, measurements of the pyroelectric coefficient and of the field dependence of the polarization.

2. CRYSTAL GROWTH AND SAMPLE PREPARATION

The crystals were grown from an aqueous solution of betaine and D_3PO_3 in a molar ratio of 1:1 by controlled evaporation at a constant temperature near 300 K. The deuteration was achieved by a three cycle process of dilution with heavy water and subsequent distillation. At least the protons of all polar bonds (those of the phosphite complex and the carboxyl group of the betaine complex) are substituted by deuterons. Thus the relevant protons of the crystal, that participate in the dipolar order-disorder phenomena, can be regarded as highly deuterated and a further deuteration of the organic complex should not affect the polar order behaviour of the system.[5] The crystals are colourless and transparent of optical quality and grow as (100)-plates with typical dimensions of about 5 × 10 × 20 mm^3. The samples were prepared as thin plates of a thickness 0.5 mm $\leq d \leq$ 1 mm and a geometrical capacitance of $C_{geo} \approx$ 0.2 pF. The measurements presented in this work have been performed with an electric field E parallel to the (010) direction. For most measurements silver paint electrodes were prepared on opposite sides of the samples. No significant difference of the results compared to those with sputtered contacts of Cr (7 nm) and Au (100 nm) have been detected.

3. EXPERIMENTAL DETAILS

In the following we give some experimental details concerning the experimental setups used for the dielectric measurements presented in this work:

i) Complex linear dielectric constant ε^*: These measurements were performed using the autobalance bridge HP4284A for frequencies 20 Hz < ν < 1 MHz and the impedance analyzer HP4191A, which uses a coaxial line reflection technique for frequencies 1 MHz < ν < 1 GHz.[12] Typical fields in these measurements were about 1 V/mm for ν < 1 MHz and 50 V/mm for ν > 1 MHz.

ii) $P(E)$ hysteresis loops and nonlinear susceptibility: For these measurements a modified Sawyer and Tower circuit has been used.[13] A reference capacitor C_r is connected in series with the sample and across this circuit a harmonic high-voltage signal is applied. Measuring the voltage across the reference capacitor and across the sample via a 14-bit multi-channel AD-device allows the phase sensitive determination of the driving field E and the polarization response P of the sample. The

Fourier-analysis of this data leads to the complex higher order terms of the field dependent dielectric susceptibility.[13,14]

iii) Pyroelectric effect: These measurements were performed using a circuit similar to that described above for the $P(E)$ loops. The reference capacitor C_r is chosen much larger than the sample capacitance ($C_r \approx 10\ \mu F \geq 10^5 \times C_{sample}$). The circuit is shorted during the cooling/heating-cycle which allows to evaluate the spontaneous polarization from C_r, the surface of the sample A_{sample}, and the measured voltage U_r across the reference capacitor: $P_s = U_r(C_r - C_{sample})/A_{sample} \approx U' C_r/A_{sample}$.

4. RESULTS AND DISCUSSION

4.1 Spontaneous Polarization and Pyroelectric Effects

The spontaneous polarization P_s of D-BPI for $E \perp (010)$ versus temperature is represented in Figure 1 (upper frame). During cooling, P_s rises markedly, signalling a ferroelectric phase transition at $T_{c2} \approx 272$ K. On further cooling, a second anomaly shows up at $T_{c3} \approx 266$ K. This second anomaly shows distinct hysteresis effects in the range between T_{c3} and 240 K, which is a fingerprint of a first order type phase transition. The temperature dependence of $\lambda = -\partial P_s \partial T$ in D-BPI (lower frame of Figure 1) can be interpreted as a superposition of two peaks, a larger one at T_{c2} and a smaller one at T_{c3} (arrows in Figure 1). This may well indicate the existence of

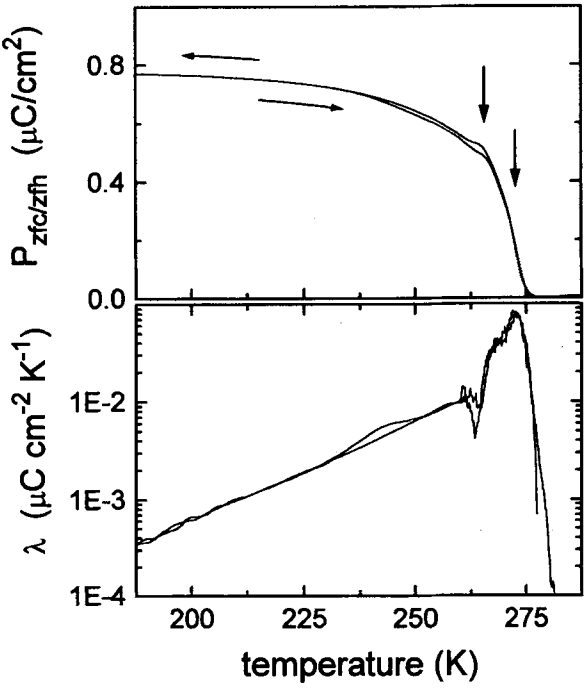

FIGURE 1 Spontaneous polarization of D-BPI versus temperature (upper frame). The data were determined with a Sawyer and Tower circuit described in the text using cooling and heating rates of 0.1 K/min. The lower frame shows the temperature dependence of the pyroelectric coefficient λ on semi-logarithmic scale.

two polar phase transitions in this temperature regime (a much smaller third peak shows up at $T \approx 260$ K, whose origin is unclear at the moment). A sequence of two phase transitions has also been found at 86 K and 81 K in BP, which becomes antiferroelectric below this temperature.[1] Possibly the second transition indicates the development of an incommensurate phase similar to the findings in betaine calcium chloride dihydrate (BCCD).[15]

For temperature smaller than 260 K, λ reveals a nearly exponential behaviour. This exponential decrease is difficult to characterize in terms of a Landau-type approach, or using laws like $P_s \propto [(T_c - T)/T_c]^\gamma$ as sometimes proposed.[4] In BA the spontaneous polarization P_s and the pyroelectric coefficient λ show a similar behaviour. Here P_s saturates at a value of 0.6 μC/cm^2 and λ reveals two peaks at 121 K and 117 K, which were ascribed to two successive FE phase transitions.[4]

4.2 Linear Dielectric Properties

In measurements of the (linear) dielectric constant of protonated BPI a peak has been found, which marks the ferroelectric phase transition.[2,3] The phase transition temperature in BPI is highly sample dependent, varying between 196 K and 220 K.[2,3] Very recently it has been reported that this anomaly is strong asymmetric and broadened[16] or even reveals a double peak structure.[11] Our results of the measurements of the complex linear dielectric constant ε^* in D-BPI for frequencies $\nu < 1$ MHz are presented in Figure 2. We find the typical peaks in ε' and ε'', which can be ascribed to a ferroelectric transition at $T_{c2} = 272$ K. However there is no sign of a second transition at 266 K as suggested by the results of the pyroelectric measurements (see above). The temperature of the FE phase transition has shifted to significantly higher temperatures compared to the protonated compound, which is due to the heavier deuterons involved in the ordering process. Aside a tiny anomaly in $\varepsilon''(T)$ at 250 K, the peaks in $\varepsilon'(T)$ and $\varepsilon''(T)$ are well defined providing no evidence for a further phase transition close to $T_{c2} = 272$ K. Only a weak dispersion and no relaxation phenomena are connected with the FE phase transition for frequencies up to 1 MHz.

As seen in Figure 2, in the temperature range between 100 K and 200 K a second phenomenon arises: The dielectric loss $\varepsilon''(T)$ exhibits a distinct maximum, which is accompanied by a small dispersive anomaly in the real part $\varepsilon'(T)$. As a function of frequency the position of this loss-maximum shifts which is characteristic for a relaxation process with a rate that slows down in the frequency and temperature range set by the experiment. Similar loss features have been detected in protonated BPI between 120 K and 190 K[11] were ascribed to a structural phase transitions. In this work also the temperature dependence of the complex dielectric constant of D-BPI has been presented for a single frequency of 5.2 kHz.[11] Here a similar anomaly near 150 K has been detected with a peak maximum in ε'' being more than one decade smaller than found in the present investigation. Possibly the field was not directed parallel to the [010]-axis as can also be inferred by the much smaller values of ε'.

To get further insight into the dynamics of the relaxational process, we plotted the measuring frequency vs temperature of the peak maximum in an Arrhenius-type representation (inset in Figure 2). Assuming a symmetric distribution of relaxation times the peak maximum in $\varepsilon''(T)$ is a measure of the mean relaxation rate $\nu(T)$ at a given temperature. $\nu(T)$ reasonably well follows a thermally activated behaviour

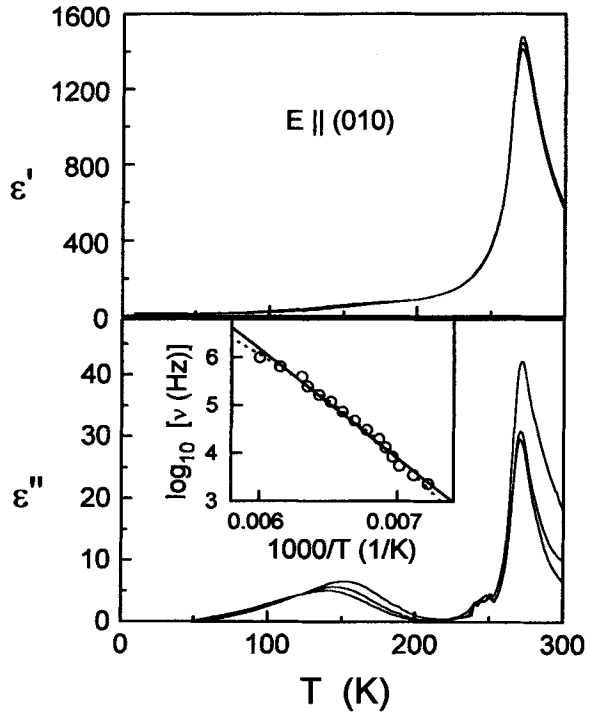

FIGURE 2 Temperature dependence of the complex dielectric permittivity ε' and ε'' of D-BPI for frequencies ν = 2.3, 13 and 75 kHz. The measurements were performed using small signal amplitudes ($E_0 \leq 1$ V/mm) parallel to the [010] direction. The inset of the lower frame shows the frequency versus the temperature of the related loss maximum between 100 K and 200 K in an Arrhenius-type representation. The solid line has been calculated assuming thermally activated behaviour with an energy barrier E_B = 5300 K and an attempt frequency $\nu_0 = 8 \times 10^{19}$ Hz. The dotted line has been calculated from a Vogel-Fulcher law with the parameters E_B = 900 K, ν_0 = 0.1 THz, and T_{VF} = 90 K.

with an energy barrier of $E_B \approx 5300$ K and an attempt frequency of $\nu_0 \approx 8 \times 10^{19}$ Hz (solid line). This unphysically high attempt frequency indicates, however, a highly cooperative process and lets expect deviations from Arrhenius behaviour at higher temperatures. These recognizable deviations from the Arrhenius behaviour can be described assuming a Vogel-Fulcher law with an energy barrier E_B = 900 K, an attempt frequency ν_0 = 0.1 THz, and a Vogel-Fulcher temperature of T_{VF} = 90 K (dashed line).

Figure 3 shows the results of the measurements of $\varepsilon^*(T)$ performed in the MHz-regime. In the upper frame the asymmetry of the peak in ε' at the lower frequencies could well be due to the two phase transitions at T_{c2} and T_{c3} as determined from the pyroelectric measurements (ν = 4 MHz (○): change of slope at 272 K and maximum at 266 K). ε' is a factor of 4 lower than in the low frequency measurements (Figure 2), which could be due to a misorientation of the crystal.

In the lower frame, $\varepsilon''(T)$ reveals a single peak structure. However, an anomaly close to 266 K can be observed at lower frequencies. With frequencies approaching the GHz-range the loss increases markedly while a double peak structure develops in $\varepsilon'(T)$. The maxima in ε'' (lower curves) indicate the condition $\omega\tau = 1$, where τ is the mean relaxation time. The inset shows the temperature dependence of the fre-

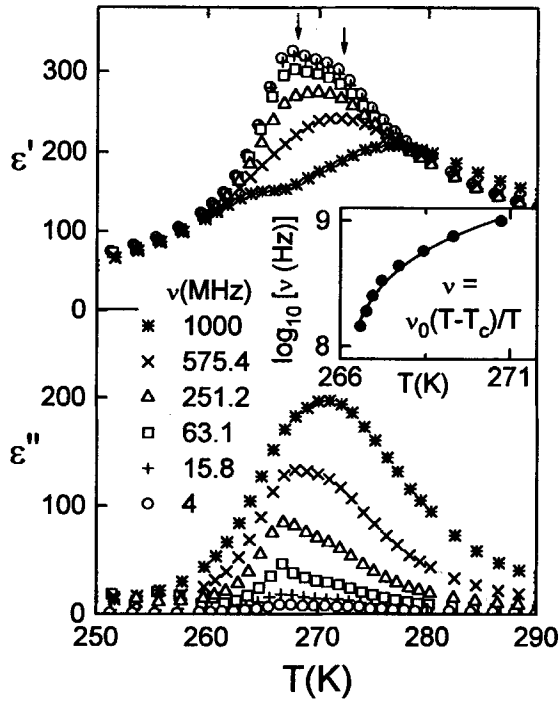

FIGURE 3 Complex dielectric permittivity ε′ and ε″ of D-BPI versus temperature in the MHz-regime (frequencies are denoted in the figure). The inset shows the relation between the frequency ν and the temperature of the loss-peak.

quency of the peak maxima. Obviously a critical slowing down of a relaxational mode can be observed at the phase transition temperature. The solid line is a fit for temperatures above T_{c3} with an expression which can be obtained from a dynamic Ising approach for order-disorder transitions,[17] namely $1/\tau \propto \nu = \nu_0(T - T_c)/T$ with $T_c = T_{c3} = 266$ K and $\nu_0 = 60$ GHz. The steep increase of the static value of the dielectric permittivity together with the critical slowing down of the order dynamics with falling temperature above the transition leads to the observed minimum in ε′ near T_c for 1 GHz.[17] Similar phenomena have also been observed in other order-disorder type ferroelectric materials as e.g. TGS, Rochelle-Salt, or KD_2PO_4.[17] (It is interesting to note that the underlying dissipation processes seem to be dominated by the transition at T_{c3} rather than by the transition at T_{c2}.

4.3 Field-Dependent Dielectric Properties

The results of $P(E)$ measurements stimulated with a harmonic field of an amplitude of 1300 V/mm are presented in Figure 4. The data are corrected for purely ohmic loss components, which are characterized by horizontal $P(E)$ ellipses. With decreasing temperature, the typical hysteresis loops show up, which indicate the development of the ferroelectric state. The temperature dependence of the parameters characterizing these hysteresis loops, such as coercive field E_c, spontaneous polarization

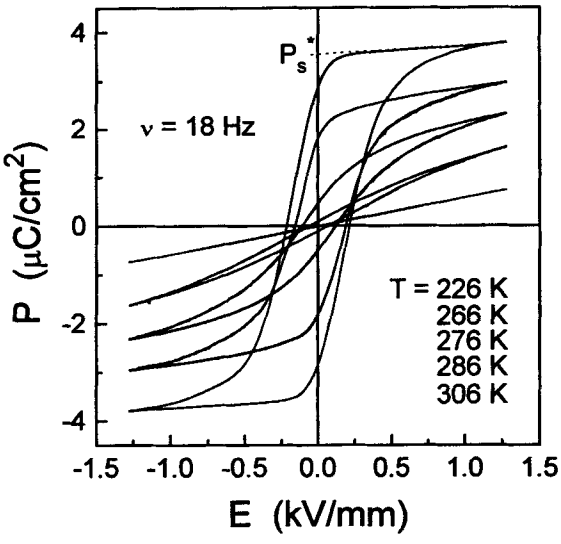

FIGURE 4 $P(E)$-hysteresis loops at various temperatures from 226 K to 306 K.

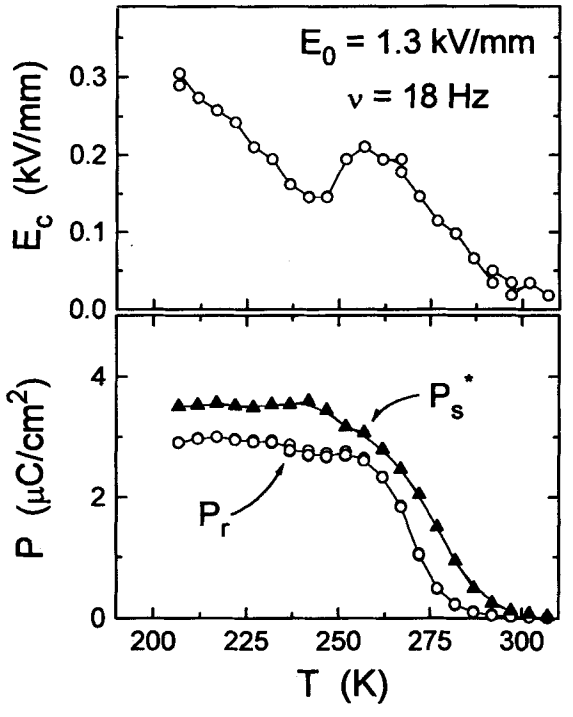

FIGURE 5 Temperature dependence of the coercive field E_c of D-BPI (upper frame), of the remanent polarization P_r and the spontaneous polarization P_s^* (lower frame) determined from the data shown in Figure 4.

P_s^* and remanent polarization P_r are shown in Figure 5. The spontaneous polarization P_s^* saturates at a value of about 3.6 $\mu C/cm^2$ below $T \approx 230$ K (lower frame of Figure 5). Saturation values of P_s^* in protonated BPI are reported to range from 1.7 $\mu C/cm^2$ to 2.3 $\mu C/cm^2$.[2,16] The coercive field E_c (upper frame of Figure 5) reveals an anomaly at $T \approx 250$ K. This unusual decrease of E_c with decreasing temperature has to be taken as evidence for a further transition, which obviously lowers the stability of the polarized domains in the crystal. To get further insight into effects connected to the stability of the ordered state, susceptibility measurements were performed using harmonic stimulation up to 167 V/mm, which is about the minimum value of E_c in the temperature range below 250 K. Results of these measurements are reported in Figure 6. The upper three pairs of frames show the linear order component of the dielectric susceptibility, χ_1, and the corresponding loss-angle, δ_1, for various field strengths and frequencies. A variety of features shows up in these data.

The peak related to the ferroelectric transition reveals a slight anomaly which increases with increasing field. Even a double peak structure develops for the loss angle at 56 V/mm at a probing frequency of 90 Hz and for χ_1 at high fields. The double peak structure probably signals the subsequent phase transitions at $T_{c2} = 272$ K and $T_{c3} = 266$ K. Just below the ferroelectric phase transition dispersion effects develop which increase with frequency. This effect indicates domain-wall relaxation processes at these relatively high fields.

The sequence of phase transitions, T_{c2} and T_{c3}, near 270 K is well documented in the magnitude of the third order susceptibility χ_3 (lower pair of frames) where a peak doublet shows up. Also the related peak in the corresponding phase angle δ_3 at 272 K seems to be accompanied by a satellite peak at 266 K.

The second feature of the data presented in Figure 6 is the existence of an additional low temperature dispersion in χ_1 (100 K $< T <$ 250 K), which is accompanied by a peak in δ_1. The position of this peak appears to be frequency and field dependent. It seems to be connected to the relaxational behaviour, observed already in the low field measurements (Figure 2). It is resonable, that for higher fields the relaxing entities stay mobile down to lower temperatures as is indeed observed in Figure 6. The evaluation of the peaks in δ_1 leads to a field-dependent thermally activated process. The corresponding effective energy barrier E_B decreases from about 5300 K for low field-amplitudes to about 2300 K with an attempt frequency $\nu_0 \approx 2 \times 10^{11}$ Hz for $E_0 = 167$ V/mm.

An additional characteristic feature in Figure 6 is a sharp jump in the third order loss angle δ_3 from a value near $-\pi$ (which denotes a ferroelectric curvature of the $P(E)$-curves with increasing field) to values near zero (which denotes the growing steepnes of the $P(E)$-curves with increasing field-magnitude in an antiferroelectric fashion) at $T \approx 250$ K. Together with the anomalies in $E_c(T)$ and $\lambda(T)$ mentioned above, the observed behaviour highly suggests the existence of a further phase transition at $T_{c4} = 250$ K. In addition there is a number of further features, which can be seen in Figure 6: i) $|\chi_1|$ shows a distinct maximum near 210 K, which is accompanied by a marked peak in $|\chi_3|E^2$. ii) There is a multiple peak structure in the magnitude of the third order susceptibility χ_3 and of the corresponding phase angle δ_3 below T_{c4}, which we found to be field-dependent. Up to now we have no explanation for these additional features but they may well reflect the complexity of the

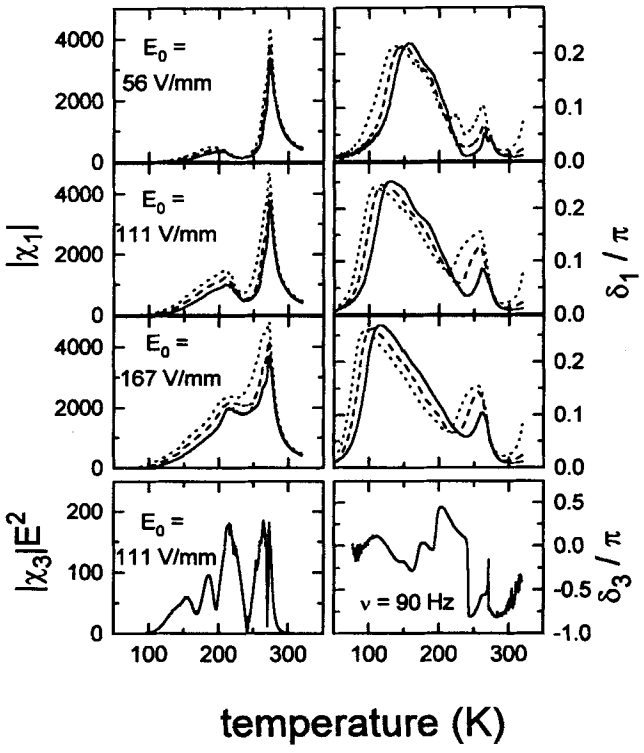

FIGURE 6 Magnitude and loss-angle of the harmonic first order susceptibility (upper three pairs of frames) of D-BPI for field-amplitudes 56 V/mm < E_0 < 167 V/mm and the frequencies ν = 0.77 Hz (dotted line), ν = 8.1 Hz (dashed line), and ν = 90 Hz (solid line) and a typical dataset of the corresponding third order terms (lowest pair of frames).

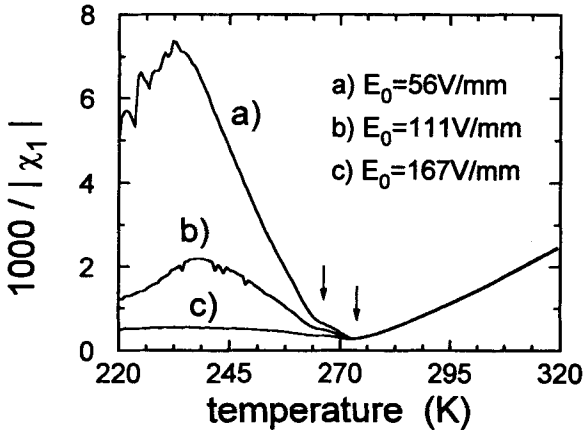

FIGURE 7 Reciprocal dielectric constant of D-BPI vs temperature at 90 Hz for various field-amplitudes. The arrows indicate the double-structured phase transition at T_1 = 272 K and T_2 = 266 K.

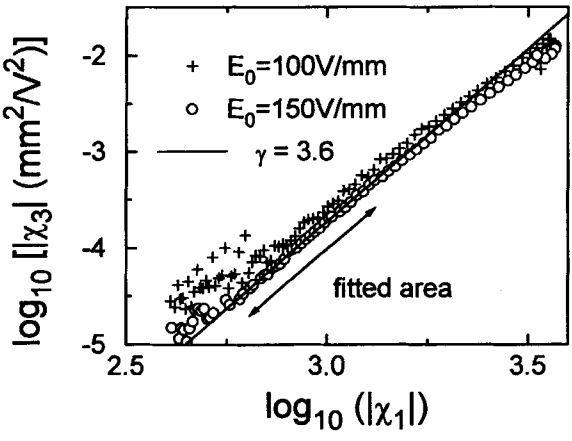

FIGURE 8 Third order vs first order component of the susceptibility of D-BPI for a frequency of 90 Hz and two field-amplitudes as denoted in the figure. The solid line with slope $\gamma = 3.6$ is the result of a fit to the marked linear area.

Figure 7 shows the $\chi_1(T)$ data of Figure 6 for a frequency of 90 Hz in a reciprocal representation. Again, the two subsequent ferroelectric transitions show up by two distinct anomalies as indicated by the arrows. The lower increase of the curves with increasing field-amplitude below T_{c3} is due to the growing coercive field. Deviations from pure Curie-Weiss behaviour close to the transition above T_{c2} can be ascribed to the anisotropy of the betaine systems.[3]

The scaling behaviour of the third order susceptibility with respect to the first order susceptibility above T_{c2} is shown in Figure 8. Following the Landau-theory for a ferroelectric phase transition, in the vicinity of the phase transition the third order susceptibility should behave like $\chi_3 = \chi_1^{\gamma}$ with a scaling exponent $\gamma = 4$.[18] Using only the strictly linear area of this double-logarithmically presented data, at least square fit (solid line) reveals a slope of $\gamma \approx 3.6$, which is close to the predicted value. From measurements of the nonlinear susceptibility in protonated BPI a value of $\gamma = 5.7$ is reported.[4]

5. CONCLUSIONS

We have performed a detailed investigation of the dielectric properties of D-BPI. D-BPI exhibits a ferroelectric phase transition which has shifted to a temperature of $T_c \approx 270$ K compared to $T_c \approx 210$ K in the undeuterated BPI. In addition indications for a sequence of three polar transitions show up at critical temperatures $T_{c3} = 272$ K, $T_{c3} = 266$ K, and $T_{c4} = 250$ K the microscopic origin of this being unclear up to now. At frequencies approaching the GHz range a critical slowing down of the order dynamics at 266 K is observed. The measurements of the pyroelectric coefficient λ revealed a nearly exponential temperature behaviour at low temperatures ($T < 260$ K). The spontaneous polarization P_s^* evaluated from hysteresis-loop measurements finally saturates at a value of 3.6 $\mu C/mm^2$, which is clearly higher than in the protonated BPI ($P_s^* = 1.7$ $\mu C/mm^2$).

We found a relaxational process in D-BPI at temperatures well below the men-

tioned phase transitions. Both, the mean relaxation rate and the energy barrier characterizing the relaxation dynamics decrease with increase field. At low fields an energy barrier of 5300 K is found. Due to its highly cooperative character, this relaxation is assumed to be related to the motion of ferroelectric domain walls.

REFERENCES

1. J. Albers, A. Klöpperpieper, H. J. Rother and K. H. Ehses, *phys. stat. sol. (a)*, **74,** 553 (1982).
2. J. Albers, A. Klöpperpieper, H. J. Rother and S. Haussühl, *Ferroelectrics*, **81,** 27 (1988).
3. I. Fehst, M. Paasch, S. Hutton, M. Braune, R. Böhmer, A. Loidl, M. Dörffel, Th. Narz, S. Haussühl and G. J. McIntyre, *Ferroelectrics*, **138,** 1 (1993).
4. M. T. Lacerda-Aroso, J. L. Ribeiro, M. R. Chaves, A. Almeida, L. G. Vieira, A. Klöpperpieper and J. Albers, *phys. stat. sol. (b)*, **185,** 265 (1994).
5. H. J. Brückner, H.-G. Unruh, G. Fischer and L. Genzel, *Z. Phys. B*, **71,** 225 (1988).
6. A. Almeida, P. Simeão Carvalho, M. R. Chaves, A. Klöpperpieper and J. Albers, *phys. stat. sol. (b)*, **184,** 225 (1994).
7. G. Schaack, *Ferroelectrics*, **104,** 147 (1990).
8. e.g. S. L. Hutton, I. Fehst, R. Böhmer, M. Braune, B. Mertz, P. Lunkenheimer and A. Loidl, *Phys. Rev. Lett.*, **66,** 1990 (1991).
9. G. J. McIntyre, M. Paasch and A. Loidl, to be published.
10. H. Bauch, R. Böttcher and G. Völkel, *phys. stat. sol. (b)*, **179,** K41 (1993).
11. H. Bauch, J. Banys, R. Böttcher, C. Klimm, A. Klöpperpieper and G. Völkel, *phys. stat. sol. (b)*, **187,** K81 (1995).
12. R. Böhmer, M. Maglione, P. Lunkenheimer and A. Loidl, *J. Appl. Phys.*, **65,** 901 (1989).
13. C. B. Sawyer and C. H. Tower, *Phys. Rev.*, **35,** 269 (1929).
14. J. Hemberger, Diplomarbeit, Darmstadt 1994.
15. W. Brill and K. Ehses, *Japan. J. Appl. Phys.*, **24,** 826 (1986).
16. R. Cach, S. Dacko and Z. Czabla, *phys. stat. sol. (a)*, **148,** 585 (1995).
17. R. Blinc and B. Žekš, "Softmodes in Ferroelectrics and Antiferroelectrics," North-Holland, Amsterdam, 1994.
18. M. Maglione, M. Lopes dos Santos, M. R. Chaves and A. Almeida, *phys. stat. sol. (b)*, **181,** 73 (1994).
19. G. Schaack, *Ferroelectrics*, **104,** 147 (1990).